Cement and Concrete Research 42 (2012) 39–50

Contents lists available at ScienceDirect

Cement and Concrete Research

journal homepage: http://ees.elsevier.com/CEMCON/default.asp

Influence of shrinkage and water transport mechanisms on microstructure and crack formation of tile adhesive mortars

A. Wetzel [a,*], M. Herwegh [a], R. Zurbriggen [b], F. Winnefeld [c]

[a] Institute of Geological Sciences, University of Bern, Bern, Switzerland
[b] Elotex AG, Sempach Station, Switzerland
[c] Empa, Laboratory for Concrete and Construction Chemistry, Dübendorf, Switzerland

ARTICLE INFO

Article history:
Received 28 January 2011
Accepted 22 July 2011

Keywords:
Cement Portland cement (E)
Polymers (D)
Failure (C)
Hydration (A)
Confocal laser scanning microscopy (B)

ABSTRACT

Shrinkage and expansion of cementitious materials like tile adhesive mortars depend on the presence of water as well as on the drying and rewetting history. Particularly for large-sized tiles such volumetric changes induce stress concentrations, which may result in cracking. This study focuses on the interplay between water infiltration and cracking, starting at the early curing of the mortar during the first days after application until water transport in the hardened system. Based on laboratory experiments, different events concerning the effect of water transport were induced by variation of the experimental setups in order to provoke cracking. Cracks at the tile–mortar interfaces suggest these domains to reflect zones of mechanical weakness. Along these cracks, water can enter the system inducing precipitation of secondary minerals in cracks and pores already after one wetting cycle. These processes reveal increasing importance during repeated cycles of drying and wetting, i.e. under outdoor conditions and may lead to failures.

1. Introduction

Cementitious tile adhesive mortars control the adhesion between tiles and substrate. Their mechanical performance is crucial for the durability of tilings on walls and floors. Application of large-sized tile formats is demanding as differential shrinkage in the tile adhesive can result in high shear stresses [1], which might provoke failures under certain circumstances. Especially the occurrence of failures on tilings faced to outdoor weathering conditions has increased in recent years [2–5]. This trend might be related to different reasons: Due to time and pricing pressure, application recommendations defined by the manufacturer often are disregarded, and low quality material is chosen. Based on market trends, larger tile formats and vitreous (non-porous) tiles are used more frequently, which enhance the aforementioned failure risk even more.

Within the system tile–tile adhesive–substrate–grout mortar, both the tile adhesive and the grout mortar build up interfaces to tile and substrate, which are supposed to represent the mechanically weakest domains. These interfaces suffer from stresses induced by differential expansion/shrinkage of the individual components of the entire system. With this respect, cementitious materials like tile adhesives may be affected by (i) capillary shrinkage, (ii) expansion due to water absorption, (iii) chemical shrinkage or (iv) thermal length changes (thermal contraction/expansion during heating/cooling).

One of the fundamental functions of a tile adhesive is to buffer the system with respect to the above-mentioned physico-chemical influences. The performance of a tile adhesive depends on the content, quality and the interaction of its components (fillers, hydraulic binders and organic binders/modifiers). Several investigations have been carried out varying the content of these components and investigating the resulting mechanical properties [6,7]. In order to evaluate the impact of certain mortar components on the mechanical properties, microstructural investigations are crucial [8]. Microstructures of polymer-modified tile adhesives have been investigated with respect to adhesion properties [7,9–13]. In those investigations, which mainly were carried out on small sized tiles (5×5 cm) applied according to European standards, the tile–mortar interface was found to be a zone, where failures often occur first. More recently, studies on large-sized tiles performed by Wetzel et al. [14] show that adhesion properties of a tile adhesive vary in respect to the position (centre vs. rim). The rim of tiles was found to be the most critical position with respect to failure evolution. As a consequence, such spatial variations in strength require spatially resolved microstructural investigations. Along the aforementioned critical position at the rim of the tile primary drying as well as potential rewetting by water intake takes place. Both drying and rewetting are coupled to a volume change, which may lead to local stress accumulations. The length changes of substrates and the surfaces of single applied tiles were measured in previous studies under wet, dry and alternating storage conditions. These measurements indicate substantial shrinkage/expansion of the system tile–tile adhesive–substrate in the range of about 0.4 mm/m. As a consequence of the stiff tile, shrinkage/expansion must lead to

* Corresponding author at: Department of Building Materials and Construction Chemistry, University of Kassel, Kassel, Germany. Tel.: +49 561 804 2603.
E-mail address: alexander.wetzel@uni-kassel.de (A. Wetzel).

0008-8846/$ – see front matter © 2011 Elsevier Ltd. All rights reserved.
doi:10.1016/j.cemconres.2011.07.007

stress concentrations at the tile–mortar interface [14,15]. The presence of water depends on (i) the curing conditions and (ii) the possibility for water to leave or enter the entire system and in particular the mortar. Both parameters are varied in this study by changing (i) storage conditions and (ii) sample setup.

In this study, we focus on the formation of initial failures, namely cracks, and water transport mechanisms, which are crucial for the failure evolution. Particularly water pathways, as there are cracks and water-induced alterations, were investigated. Using an experimental approach, a special setup of single applied large porcelain tiles, which were applied on a concrete substrate with a polymer modified tile adhesive, allows investigating (i) a "real" system under laboratory conditions and (ii) spatially resolved sampling to track down cracks and secondary formed minerals. Variation in climatic laboratory conditions enables the simulation of failure evolution mimicking outdoor weathering. Parallel to the present study investigations on a field-experiment with entire applied tilings, in parts faced to natural weathering conditions, were carried out [16]. Macro- and microstructural observation of that study confirms the assumption that the chosen setup of single applied tiles can in parts be assigned as a simulation of the field case. However, the evolution of failure is closely related to the question whether water is mainly transported along capillaries or along pathways like mortar internal or interfacial cracks. To identify the initial locations of such cracks, spatially resolved sampling for microscopic investigations was performed.

2. Experimental approach

2.1. General setup

In three different experimental setups large-sized porcelain tiles (30×30×0.8 cm, type BIa according to EN 14411) were applied on a concrete substrate (40×40×4 cm, Antoniazzi, type RUEN, according to EN 1323), using a standard test formulation of tile adhesive.

In the first setup, extreme conditions in terms of drying and rewetting are provided due to open flanks of the applied mortar, as no grouts were applied. The rear side of the tile was abraded prior to applications to remove a white engobe and the topography gaining a homogeneous even surface at the tile's rear side. This engobe is mainly composed of magnesium oxide and originates from a slurry applied by the tile manufacturer to prevent adhesion of the tile on the band conveyor during the firing process [9]. Sample NG (Table 1) was prepared with this setup, which is described in detail by Wetzel et al. [14].

In a second setup, additional tile fragments were applied on the remaining surface of the concrete substrate outside the large tile (Fig. 1). The joints between the large tile and the tile fragments were closed by applying grout mortar. The rear sides and side faces of the concrete substrates were sealed with a two-component adhesive prior to application to prevent drying along these sides. The rear sides of the tile were cleaned prior to application using a high-pressure cleaner to remove the white engobe, which might influence the adhesion behaviour of the tile [16]. Samples CO1 and CO2 were prepared according to this second setup (Table 1). Sample FW is considered as third setup, which is similar to the second setup, but in addition the substrate was covered on top with a one-component flexible waterproofing one week prior to application of the tile adhesive.

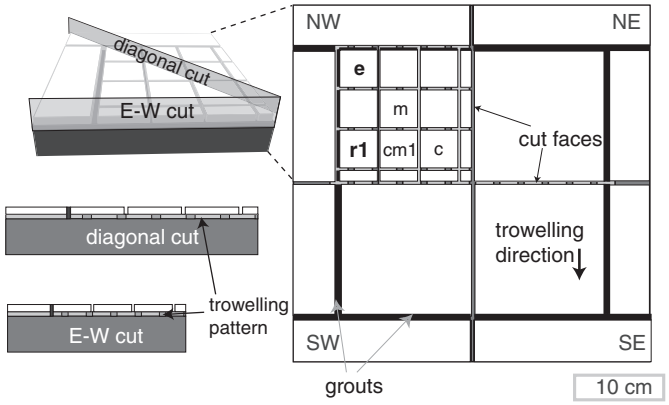

Fig. 1. Sample assemblage and sampling positions for microstructural analyses in a diagonal and an E–W cut. (N–S corresponds to the direction of mortar trowelling.) The labelling code for the different positions (e = edge, m = middle, c = centre, r1 = rim position 1, cm1 = between centre and middle position 1) was defined by Wetzel et al. [14].

With these three experimental setups different water transport mechanisms and their influence on the microstructural evolution of the tile adhesive can be compared. Based on (i) the different setups, (ii) storage conditions and (iii) specific sampling positions (Fig. 1) we defined a labelling system for the samples described in Table 1. A thin-section, for instance, positioned at the rim (e or r1, see Fig. 1) on the sample with the flexible waterproofing, sampled after 56 days of dry storage (23 °C/50% rel. hum.), would be labelled as FW-dry_rim.

One quadrant of samples FW, CO1 and CO2 was used to investigate the failure mechanisms occurring under wet conditions. To ensure that water only could enter the system along the grouts a special setup was developed. A plastic frame was fixed on top and along the side faces of the quadrants with silicone sealant forming a basin. Then water was poured into the basin to allow water ingress along the grouts for a time period of 42 days. Note that water ingress in all three samples can only have been occurred over the grouts, which

Table 1
Samples and analyses.

	Sample label	NG (no grout)		CO1 (concrete)			CO2 (concrete)			FW (flexible waterproofing)		
Setup	Stained Additive	none		CE			Latex			PVA		
	Treatment of tiles backside	abraded		wet cleaned high pressure						wet cleaned high pressure		
	Treatment substrates backside	no		sealed with two component adhesive						sealed with two comp. adhesive		
	Application of grouts	no		yes						yes		
	Fexible waterproofing	no		no						yes		
Storage	Sampled quadrant *(see Fig. 1)*	NW	SE	NW	NE	SE	NW	NE	SE	NW	NE	SE
	Dry (23°C / 50% r.H.) [days]	7	7	56	160	190	56	160	190	56	160	190
	Wet (grout moistening) [days]					42			42			42
	Wet (water immersion) [days]		450									
Analysis	Optical microscopy (thin sections)	E-W	E-W			E-W			E-W	diagonal		E-W
	LSM (polished sections)			diagonal	E-W	E-W	diagonal	E-W	E-W	diagonal	E-W	E-W
	Thermogravimetry		N-S	E-W		E-W				E-W		E-W
	SEM (fractured surfaces)		E-W									

represents a first scenario. In contrast, sample NG represents a second scenario, where water can also infiltrate along the open flanks during immersion over a time period of about 450 days of the entire setup into a water tank. The first scenario is representative for outdoor tile floors while the second scenario reflects extreme outdoor conditions or situations typical for swimming pools.

2.2. Mortar formulations and staining of additives

The formulation of the used tile adhesive (Table 2) contains Portland cement (CEM I 52.5 R), fillers (quartz, dolomite), an organic binder (latex) and an organic modifier (cellulose ether). The cellulose ether (CE) achieves thickening, entrainment of air and water retention. The organic binder commonly is added to the dry mix as redispersible powder. The redispersible powder is gained by spray drying. During this procedure polyvinyl alcohol (PVA) is added to stabilise these particles. This powder redisperses in water and forms latex films during drying. The tile adhesive corresponds to a C2 quality according to EN 12004.

The used grout mortar is commercially available and corresponds to the type CG2 according to EN 13888. A standard flexible waterproofing for applications compliant with moisture resistance classes A01, A02 and B0 [17] was applied.

Polymers commonly used in tile adhesives are very difficult to be localised and quantified in the microstructure by conventional analytical methods because of (i) dissolution and/or mobilisation during sample preparation and (ii) limited resolution of conventional analytical methods (e.g. optical microscopy). For that reason, we followed an approach developed by Jenni et al. [11] and DeGasparo et al. [18], which guarantees the stability of polymers during sample preparation and enables the localisation and the quantification of the relative distribution of the polymers by confocal laser scanning microscopy (LSM).

For this approach, the individual polymers were stained with the fluorescent dye fluorescein thioisocyanate (FITC) prior to mortar mixing. Polyvinyl alcohol (PVA) and cellulose ether (CE) were stained following the instructions of Jenni et al. [11]. Fluorescein acrylate monomer (0.04 g fluorescein o-acrylate 97%, Sigma-Aldrich per 100 g polymer) was added during polymerisation of a polyvinyl alcohol stabilised vinyl acetate/vinyl versatate/butyl acrylate terpolymer.

For the fresh mix of the tile adhesive the stained polymers and other liquid polymer dispersions are added to the water (Table 2). Afterwards, the dry mix is added to the water–polymer mixture, while stirring for one minute with a propeller mixer (Ø 80 mm, mixing speed of 750 rpm). The mortar is applied on the substrate and is combed from north to south (in respect to the substrate, see Fig. 1) by a notched flow bed trowel (7.3/12/20 mm) keeping the angle between trowel and substrate constantly at 60°. Owed to the geometry of the trowel, the mortar forms ribs proceeding from north to south. When the tile is placed on the mortar, the ribs are pressed down resulting in an enhanced contact area between tile and mortar. A more detailed description of the mortar mixing and application procedure is given in Wetzel et al. [14].

Table 2
Formulations and type of stained additive used in different setups (NG, CO1, CO2, FW, see Table 1). *s.c. = solid content.

		Sample/formulation			
		NG	CO1	CO2	FW (wt.%)
Dry mix	CEM I 52.5 R	35	35	35	35
	Quartz sand 0.1–0.6 mm	15	15	15	15
	Quartz sand 0.1–0.3 mm	32	32	32	32
	Dolomite powder	15	15	15	15
	Unmodified cellulose ether	0.4		0.4	0.4
	Redispersible polymer powder (latex)	3.0			
Fluid/dispersion	Latex (s.c. 53.6%)		4.42		4.42
	PVA (s.c. 24.25%)		0.30	0.30	
	Stained PVA (s.c. 1.93%)				3.73
	Stained CE (s.c. 2.62%)		15.09		
	Stained latex (s.c. 39.23%)			6.03	
	Water	25.00	6.03	19.11	16.04

2.3. Sample preparation

After predefined dry or wet storage conditions (Table 1) the samples were cut along N–S and E–W direction (Fig. 1). The resulting four quadrants are mirror images and therefore, only one quadrant needs to be sampled for microstructural investigations, while the three remaining quadrants were sealed again and were stored under different storage conditions for further investigations (Table 1).

Different positions can be sampled to gain profiles from centre to rim (diagonal or E–W/N–S). The edge position (e) is exposed by two sides to the grout and is thus of special interest. A cut from the edge to the centre (diagonal cut) also cuts the ribs of the mortar diagonally, which are aligned from N to S due to the trowelling direction (Fig. 1). In addition cuts in E–W direction (equatorial cuts) were made at a 90° angle to the trowelling direction.

The different cross-sections were used to prepare (i) thin-sections (optical microscopy, scanning electron microscopy), (ii) polished sections (confocal laser scanning microscopy), and (iii) samples for thermogravimetric analyses (see Table 1). To avoid failure and debonding of the tile during sawing, the entire quadrant was embedded first in an epoxy-based resin. All sawing works were carried out under dry conditions to avoid secondary hydration or dissolution of components due to potential exposition to cooling water.

The samples used for preparation of thin-sections (25 μm thick) were first impregnated with an epoxy-based resin stained with blue pigment in low vacuum. In the final step during thin-section preparation a transparent resin was used. Inhomogeneities in some samples may occur at locations where the coloured resin was not distributed homogeneously over the entire thin-section.

Polished-sections were prepared with polyfin as resin, as described by Jenni et al. [11], to avoid dissolution of polymer components of the tile adhesive. The visualisation and imaging of polymer distribution was carried out on polished-sections using a confocal laser scanning microscope (LSM 5 Exciter, Carl Zeiss Microimaging GmbH, Jena) with an Ar-Laser (488 nm). Several mosaic pictures, stitched automatically, were obtained keeping following parameters fixed: stack size, 643.3×643.3 μm, 512×512 px; pixel size, 0.8 pixel/μm; scan time, 12.8 μs/px; objective, ec Plan-Neofluar 10×/0.30m27_1; filter, low pass 505; transmission, 10%; pinhole, 70 μm; beam splitter, MBS: HFT 405/488.

For the quantification of the polymer distributions in sections across the mortar, the grey values of each pixel of the stitched pictures were read out and summed up along horizontal stripes following the approach described by Jenni et al. [11]. Thereby the signal was corrected for background, quartz grains and pores. The local grey values are then correlated with the vol.% of certain polymers assuming the bulk intensity corresponds to the total amount of stained polymer. For analysis of microstructures on thin-sections, polished-sections or fractured surfaces were analysed by scanning electron microscopy (SEM) using a Zeiss EVO-50 XVP.

Thermogravimetric analyses (TGA) were carried out in order to identify the local occurrence and quantity of hydrates, organics, portlandite and carbonates. The tile adhesive was sampled along a thin stripe of about 1 cm thickness using an ordinary metal saw. This stripe provides a profile from centre to rim in an E–W or N–S cut. The about 2 mm wide notch, which was gained by the saw, delivers about 100 mg of mortar for the TGA. This amount was analysed on a TGA/SDTA 851e from Mettler Toledo using 150 μl platinum crucibles.

Under air conditions the samples were measured at a heating rate of 10 °C per minute up to 1000 °C.

3. Results

3.1. Microstructural analysis

3.1.1. General observations

Conventional optical microscopy was used to analyse microstructures in the major components as there are porcelain tile, tile adhesive, flexible waterproofing, concrete substrate and grout mortar (Fig. 2). Within the mortars (tile adhesive and grout mortar), one can distinguish between matrix (consisting of fine fillers and hydrates), coarse fillers (quartz) and pores (Fig. 2c). The rib positions can be located easily in case of rim positions due to the fact that at these positions a hollow exists because of the discontinuous contact between tile and tile adhesive [14]. The ribs were not sheared completely during tile inlaying and the flanks of these ribs are now visible in the cross-section. In one thin-section, such a hollow between tile adhesive and tile was filled with grout mortar (Fig. 3a, left side). This thin-section was derived from the edge position from a diagonal cut of a quadrant and therefore grout mortar entered the hollow parallel to the ribs. On E–W cuts, on the contrary, no grout mortar was pressed in and the hollow between the outermost and the following rib remains unfilled (Fig. 4). Generally, the microstructure within the tile adhesive is affected by external forces during inlaying of the tile. Using an inlaying-gauge and a constant load of 33 kg guarantees that the external forces are kept identical during application of the tile (for details see Wetzel et al. [14]). Hence any microstructural variation in the mortar between the different experiments must be related to differences in storage conditions and positions within the sample and not to preparation artefacts. The shearing of mortar ribs during inlaying of the tile and resulting structures are discussed in detail by Wetzel et al. [14].

A tile adhesive is a porous material, as during the mixing process of the fresh mortar air is entrained. Pores of a size between 20 and 600 μm, so called air voids, make up a volume of about 25% of the mortar. In addition, also smaller pores exist in the mortar matrix in form of capillary and gel pores. Some air pores located at the tile–mortar interface show a low opening angle between tile and air–mortar interface (Fig. 4). These pores originate from air voids entrapped during inlaying of the tile. The entrapped air voids mainly accumulate along positions, which can be assigned to former rib positions. This finding confirms macroscopic observations in experiments, in which glass plates instead of tiles were applied. Here, traces of air voids can directly be correlated with former rib positions [14]. On the contrary, air voids entrained during mixing of the fresh mortar are generally round-shaped and the air–mortar interface is steeply inclined with respect to the tile. These pores can also become deformed during inlaying of the tile. Another type of pores locally occurs at the interface of tile and grout mortar (Figs. 3a and 4b), which differs in appearance to entrained or entrapped air voids. These so called “dead end pores” occur as a row of symmetric pores at the border to the tile. They originate from water trapped during grout mortar application.

A thin layer of engobe interrupts the interface between the dense porcelain tile and the porous mortar. In the case of samples CO1, CO2 and FW remnants of this magnesium oxide exist, despite prior cleaning with high pressure. The contact between tile adhesive and concrete substrate, respectively the flexible waterproofing in case of sample FW, can clearly be followed (e.g. Fig. 4a).

3.1.2. Crack patterns

Along diagonal (e, m, c) or E–W-cuts (r1, cm1, c) a profile from rim to centre of the tile can be studied in terms of the location and frequency of cracks. In the following, observations from light microscopy on thin-sections located at the rim (e, r1) of the tiles are illustrated (Figs. 3–6). Rim positions (e, r1; see Fig. 1) are

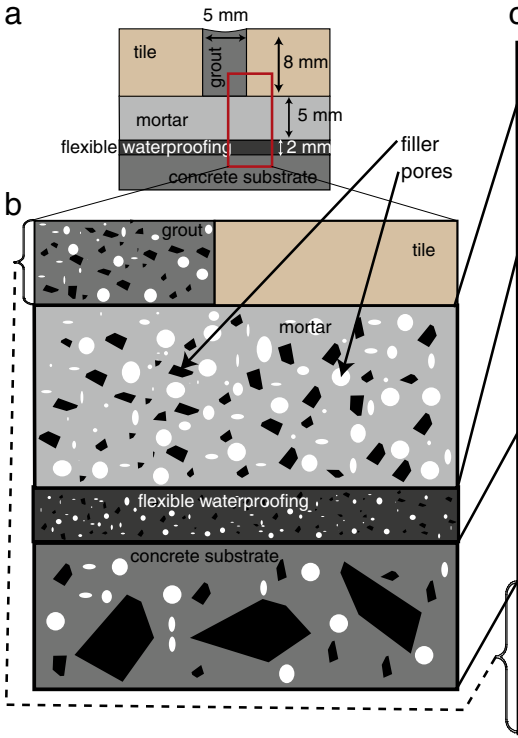

c

material	component	mineralogy	size	content [vol.%]	comments
tile adhesive mortar	coarse filler	quartz	20-600μm	30	
	pores	-	20-600μm	25	capillary and gel pores (not locatable)
	matrix	hydrates, dolomite (fine filler)	-	45	polymers (not locatable)
flexible waterproof.	coarse filler	quartz	20-250μm	15	-
	pores	-	20-250μm	25	-
	polymer matrix	-	-	60	hydrates and fillers occur as inclusions
concrete	coarse filler (aggregates)	polymineralic (granit, carb. , etc.)	250μm-20mm	50	-
	pores	-	20-500μm	7.5	-
	matrix	hydrates	-		div. fine g. fillers
grout	coarse filler	quartz	20-500μm	25	
	pores	-	20-500μm	15	capillary and gel pores (not locatable)
	matrix	hydrates, carbonates (fine fillers)	-	60	polymers (not locatable)

Fig. 2. (a) The sample consists of tile, tile adhesive, flexible waterproofing, concrete substrate and grout mortar. (b) Besides the tile all components are cementitious composites containing filler (black), matrix (different grey values) and pores (white). (c) Sizes and content of the individual components are listed.

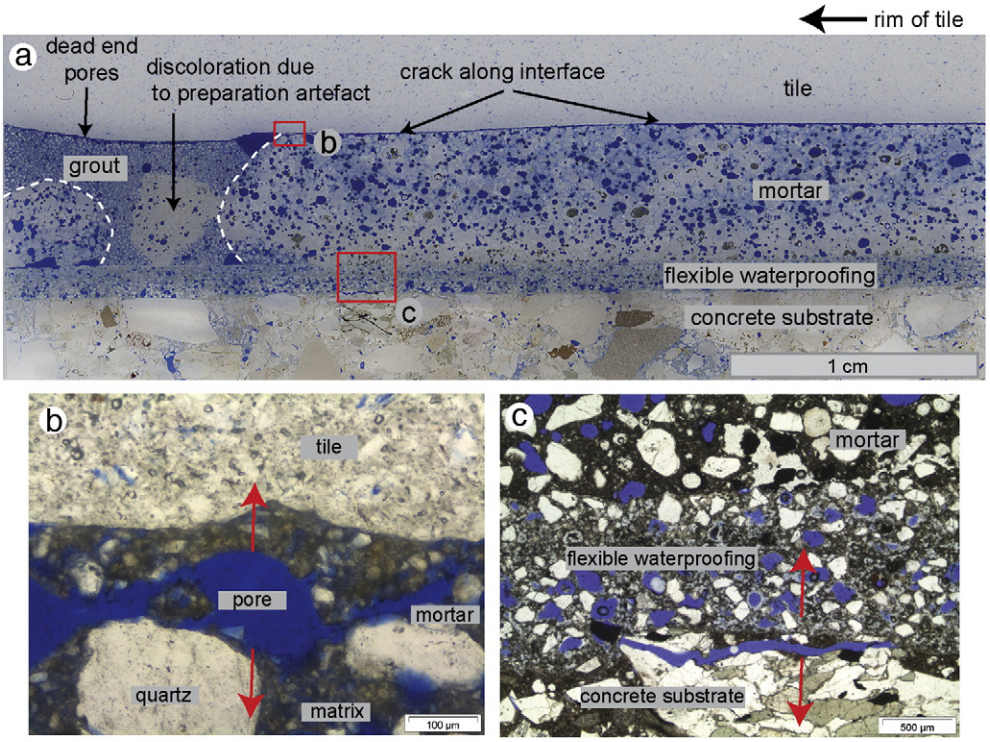

Fig. 3. (a) Overview of the thin-section FW-dry_rim. Details of horizontal cracks (b) at the interface between tile and mortar and (c) within the substrate in direct vicinity to the flexible waterproofing.

supposed to represent domains of most pronounced mechanical contrast in microstructure. A detailed description follows below. In the following, results mainly of sample NG (dry and wet) and sample FW (dry and wet) are shown and compared to each other. Results of samples CO are almost similar to those of FW due to small differences in sample setups two and three (see above).

In order to characterise microstructures related to dry and wet storage thin-sections were mapped (Fig. 7) to investigate the

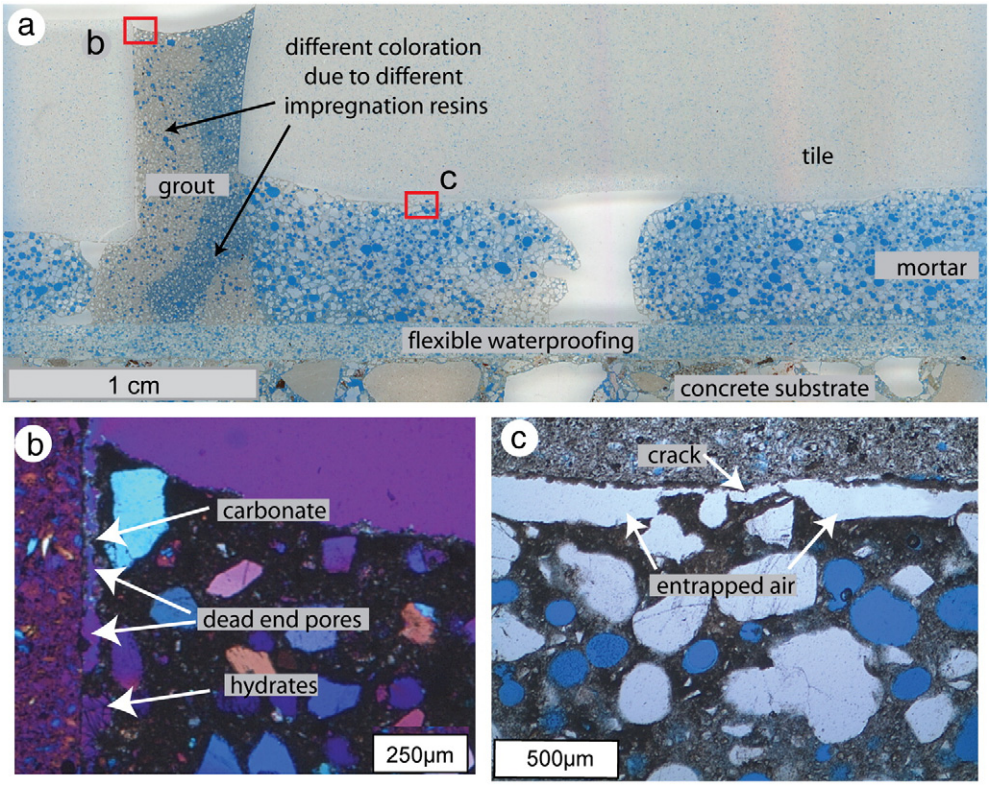

Fig. 4. (a) Thin-section overview of sample FW-wet_rim (wetted along the grout). (b) Carbonates and hydrates along vertical cracks following dead end pores (arrow) at the tile–grout interface. (c) Cracks and entrapped air voids along the horizontal tile–mortar interface.

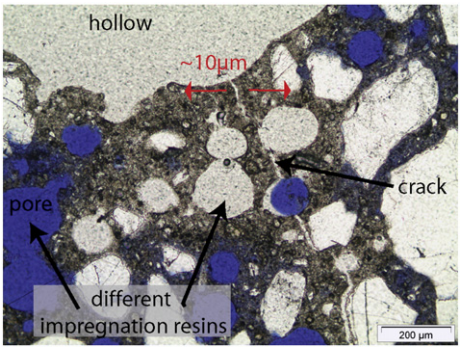

Fig. 5. Crack at a rim position in a dry stored sample preferentially follows interfaces of coarse filler grains (NG-dry).

distribution of (i) cracks within the mortar (blue) and along its interfaces (green), (ii) entrapped air voids (yellow) and (iii) the formation of secondary minerals (carbonates in purple, hydrates with different sizes in different symbols).

In general, two types of cracks can be distinguished: (i) Cracks at the interfaces of all used materials and (ii) cracks within the tile adhesive or the grout mortar (vertical cracks). Cracks at the interface seem to propagate preferentially along entrapped air voids or dead end pores (Fig. 4). Occasionally, interface cracks propagate away from the contact into the mortar continuing there as mortar internal crack. Mainly such crack propagation into the mortar bed occurs at the locations where remnants of engobe are still present. A mortar internal crack might proceed through the entire mortar bed or may end within it.

3.1.2.1. Interface tile–tile adhesive. A crack at the tile–mortar interface was observed on the dry stored sample FW-dry (Fig. 3) following the entire interface reaching about 8 cm into the tile's centre (on another thin-section). At this position, the crack proceeds into the mortar with an angle of about 60° ending just above the flexible waterproofing. Cracks at the tile–mortar interface were also found on the sample FW-wet, which was wetted along the grouts (Fig. 4). Those cracks were interrupted and are therefore not continuous like those of the dry stored sample (FW-dry). Nevertheless, both samples (FW-dry and FW-wet) are comparable in terms of crack width (Fig. 7a,b).

3.1.2.2. Interface tile–grout mortar. Also along the interface between tile and grout (flanks) cracks were observed in sample FW-wet_rim (Fig. 4). There is a thin crack with a maximum width of 10 µm at the right side (side of the large tile) and a larger crack with about 35 µm width at the left side (side of the small tile, see also Fig. 1 for comparison with the setup). The latter follows the entire interface interconnecting dead end pores (Fig. 4b).

3.1.2.3. Interface tile adhesive–flexible waterproofing. The interface between concrete and flexible waterproofing also shows several cracks. These cracks are not located at the interface itself but occur within the concrete. Note that they even cross cut mineral components (Fig. 3c). Such cracking of mineral components in the substrate indicates a good adhesion between flexible waterproofing and substrate. The crack width varies between 20 µm and 50 µm. In sum about 20% of these interface areas show these cracks.

3.1.2.4. Mortar internal cracks. Cracks within the mortar occurred in samples with abraded rear sides of tiles (Figs. 5 and 6). Those cracks proceed almost perpendicular to the tile and initiate mainly at hollows (uncontinuous contact between tile and mortar) and pores. Cracks within the mortar often follow along the surfaces of larger-sized (coarse) filler grains (Fig. 5). In some cases they continue through almost the entire mortar bed. These cracks never reach the tile–mortar or mortar–substrate interfaces (Fig. 7c). The widths of such individual vertical cracks vary from ~1 µm to ~15 µm. Within one thin-section of the dry stored sample (NG-dry), measuring 4 cm in length, a summed-up crack width of about 15 µm was estimated.

A sample of the same setup type was stored in water for 450 days (NG-wet). Along a profile from centre to rim three thin-sections were mapped. In the thin-section located at the rim, a maximum crack width of 15 µm was observed (Fig. 7). Towards the centre of the tile, crack widths of 1–5 µm occur at periodical distances. The summed-up crack widths for single thin-sections are comparable for the three thin-sections from core to rim. All cracks over the three thin-sections reflect an accumulated width of ~100 µm, which can be transferred over the 12 cm of the three thin-sections to a general mortar-shrinkage of 0.8 mm/m.

3.1.3. Secondary formed minerals

During the hydration process the clinker phases in the Portland cement react to hydrates. Within the cement matrix, the size of these

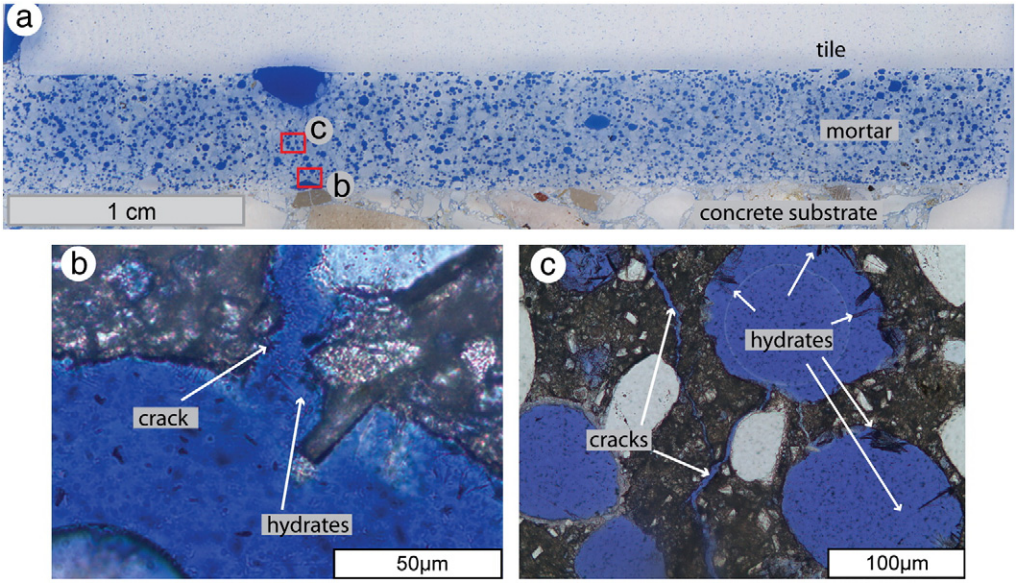

Fig. 6. (a) Thin-section of sample NG-wet_rim. (b) Hydrates formed within a crack, which ends in a pore. (c) Secondary formed hydrates in pores in the vicinity of cracks.

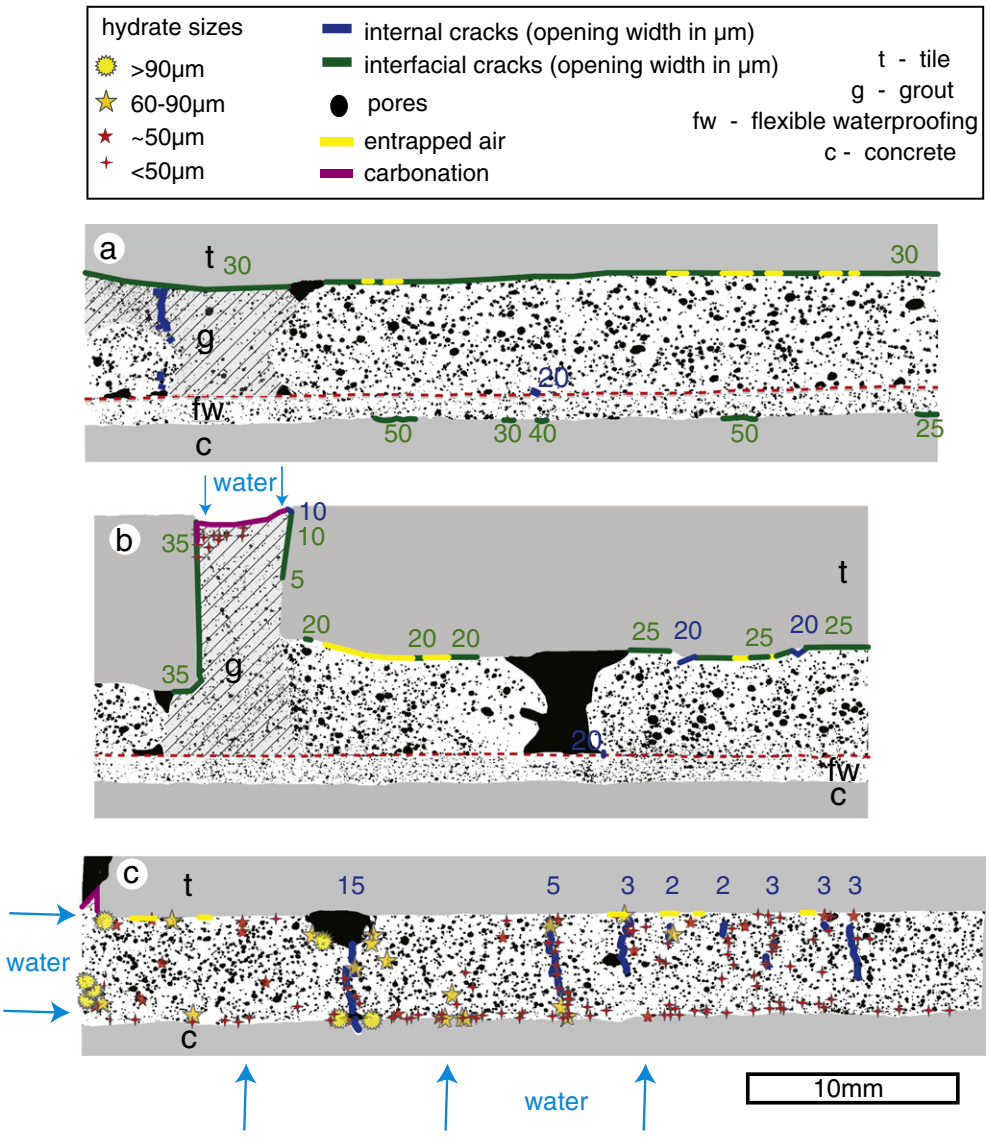

Fig. 7. Mapping of thin-sections of peripheral samples: (a) 8 weeks dry stored sample (FW-dry_rim), (b) sample wetted over grout during 6 weeks (FW-wet_rim) and (c) sample immersed in water tank during 450 days (NG-wet_rim).

primary formed minerals usually is too small to allow an identification of these phases based on optical microscopy.

A significant amount of secondary formed minerals can be observed in the case of the sample NG-wet stored in a water tank over a time period of 450 days. In contrast, samples wetted only along the grout for a short time period of 42 days only show a small amount of secondary formed minerals within the grouts itself. The occurrence of secondary formed minerals is associated with the appearance of cracks. These cracks either follow the interface (samples CO-wet and FW-wet, Fig. 4b) or are located within the mortar (sample NG-wet, Fig. 6b,c). On the walls of the cracks and the walls of the pores located near these cracks new hydrates are formed. The mappings of cracks and hydrates clearly show that the local occurrence of both structures correlates (Fig. 7b,c). The size of the hydrates varies. A maximum size of 160 µm was observed for hydrates situated at the rim of the sample stored over 450 days in a water tank (NG-wet). Towards the centre of the sample the size of the hydrates decreases (Fig. 7c).

Hydrates either can be ettringite (needles) or calcium hydroxide (platelets). Both occur in assemblages and can hardly be discriminated form each other by light-microscopy. Fractured surfaces of cross-sections of the wet stored sample (NG-wet) were studied with scanning electron microscopy. Due to the grain morphologies, ettringite clearly was discriminated from calcium hydroxide (Fig. 8a). This differentiation was confirmed by element mappings using energy dispersive spectroscopy (EDX).

Beside hydrates also secondary carbonates are formed due to wet storage and CO_2 ingress leading to the formation of a carbonated skin on the top of the grout in the wet stored samples (FW and CO). Additionally, also upper parts of cracks (400 µm deep) along tile–grout interface show carbonation (FW-wet, Fig. 4b). At the rim of sample NG-wet carbonates and hydrates are observed by SEM at the tile–mortar interface along the side faces of the tiles (Fig. 8b). These cracks filled with secondary minerals (e.g. carbonates) measure widths of about 20 µm and follow the side face of the tile as long as mortar is in contact to the tile.

3.2. Spatial distribution of polymers

Fig. 9 shows the distribution of stained polyvinyl alcohol (PVA), cellulose ether (CE) and latex, each distribution after 160 days of dry storage (a, c, e) and additional 42 days of wet storage (b, d, f). Compared to the fluorescence intensity of the FITC dye attached to the

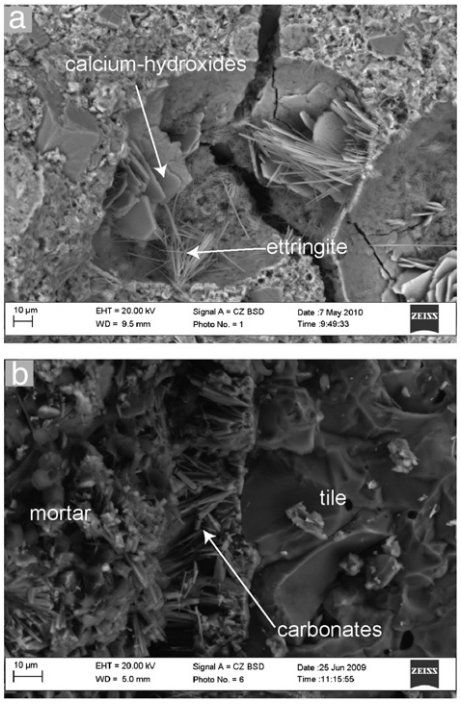

Fig. 8. (a) Hydrates (ettringite needles and calcium-hydroxide platelets) in an entrained air pore. (b) Secondary formed carbonates and hydrates along vertical tile–mortar interface.

polymers, a low fluorescence signal of the mortar itself can be measured. Note that this fluorescence is quite weak and can be neglected, as can be seen in a comparison between the non-stained grout mortar and the tile adhesive (Fig. 9). Note that single darker areas, like in Fig. 9c, could be related to material transport perpendicular to thin-section area.

The polymer distribution is quantified from the rim to the centre of the tile system. Since the central positions show homogeneous distributions for all three polymers and the major fluctuations occur in the rim regions only, we will focus on the latter (Fig. 9).

PVA and CE are enriched along the contact to the grout. A thin skin of about 50 µm thickness was observed. Along the surface of the mortar to the hollow none of these enrichments occur. Note that no stained polymers have migrated into the grout.

The latex shows a homogeneous distribution in horizontal as well as in vertical direction. Local enrichments can be interpreted as aggregates of latex particles or large latex films. Former investigations already found that CE and PVA are water-soluble and can be transported through mortar capillaries [11]. Enrichments at the interface between tile adhesive and substrate in the case of a substrate with a high water absorption capacity were found. Latex particles probably are too large (about 1 µm) to be mobilised by capillary water transport, which is confirmed by former investigations [19]. The wet storage does not alter the polymer distribution.

Beside the aforementioned horizontal concentration gradients of PVA and CE at the contact to the grout mortar, also vertical gradients within the tile adhesive bed can be observed. On samples located at the centre of the tile, these gradients were quantified. The resulting quantification indicates that the PVA is depleted near the substrate, which does not absorb water (Fig. 10), while CE is slightly enriched towards the substrate. The latex shows a homogeneous distribution. Keep in mind that in the case of CE and PVA water absorbing and waterproofing substrates are used, which can affect the migration of water and therefore also the migration of dissolved polymers (see discussion).

3.3. Spatial variation in degree of hydration

In order to quantify the content of hydrates, the tile adhesive was locally sampled after dry and wet storage and measured by thermogravimetric analysis. The weight loss in the TGA curve between 430 °C and 480 °C is characteristic for the dehydration of portlandite, and can therefore be used as an indicator for the degree of hydration [19].

All samples (except sample NG-wet) show an increase in portlandite content towards the centre (Fig. 11), while a depletion of portlandite can be observed in the outermost 4 cm.

Sample NG-wet shows the highest values over the entire profile. At the rim it even reveals a slight increase indicating a higher degree of secondary hydration due to availability of surrounding water. This enhanced degree of hydration was also observed by mapping of thin-sections using light-microscopy. A larger amount as well as bigger crystals of portlandite and ettringite occurs within the pores towards the rim of the tile (Fig. 7).

For all other samples, grouts were applied one day after application. Samples CO-wet und FW-wet were wetted over the grout. Portlandite contents, however, are similar to the dry stored samples, indicating that no water entered within these 42 days. The portlandite contents in the centre (max. distance to the rim) are higher for the almost non-absorbing sample FW with flexible waterproofing compared to the samples with no flexible waterproofing (CO1, CO2).

4. Discussion

Based on the described experiments the water regime and associated water transport mechanisms and pathways for drying and rewetting will be discussed in the following.

4.1. Processes related to primary drying

Principally, the drying processes in the mortar start directly after application affecting capillary shrinkage, while the remaining water reacts with the cement to hydrates resulting in chemical shrinkage. Chemical shrinkage describes the volume decrease due to the formation of hydrates from the anhydrous cement [20,21]. No significant external length reduction of the mortar is caused by chemical shrinkage. Rather, additional gel-porosity is formed, reducing the mean pore radius. The reduced pore sizes enhance capillary shrinkage, when the system is drying out, as a higher capillary tension is created. Thus, an increasing degree of hydration indirectly increases the volume changes due to water absorption and drying processes. Capillary shrinkage describes the physical discharge of water driven by evaporation or uptake by a substrate [22]. Slowik et al. investigated early age shrinkage (few hours to one day) on cement-based materials [22]. It is mainly affected by evaporation. Chemical shrinkage can be neglected in this period of mortar curing [23].

Transferred to our experimental setups, the mortar can dry (i) along the flanks and the substrate driven by evaporation and soaking, respectively (sample NG, Fig. 12a). (ii) In the case of samples CO, where the substrate is sealed on bottom and side faces, the mortar can dry along the grout by evaporation and in parts over the substrate (Fig. 12b). (iii) In the setup a flexible waterproofing is applied on the top of the concrete substrate, i.e. sample FW, the mortar can only dry along the grouts (Fig. 12c). The difference in vertical distribution of CE and PVA as water-soluble polymers shows that the sample with flexible waterproofing represents an almost non-soaking substrate resulting in enrichments in the upper 2/3 of the mortar bed (Fig. 10a). In contrast, the substrate without flexible waterproofing (samples CO, Fig. 12b) is soaking as indicated by the enrichments of CE towards the substrate (see also Jenni et al. [19]).

The volume changes owed to drying and hydration of the mortar during curing lead to local stress accumulations, which can result in

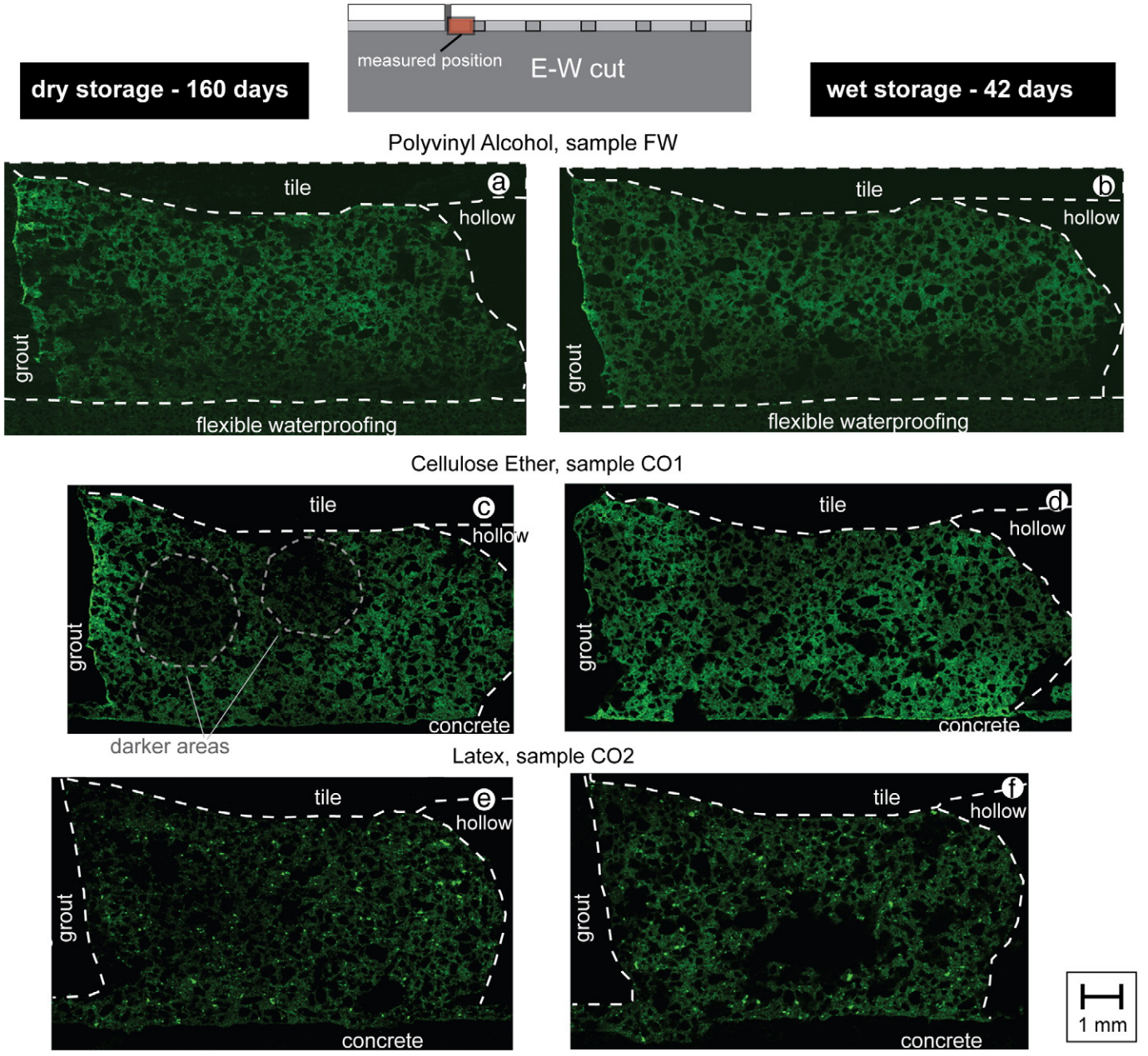

Fig. 9. Spatial distribution of stained polymers (PVA, CE and latex) in mortar at the rim of the tile in direct contact to the grout (left side) tile (top), hollow (right side) and substrate (bottom) after dry (a, c, e) and wet storage (b, d, f).

adhesion or cohesion failure at peculiar sites. These failures were observed in form of cracks at the interfaces (adhesion failure) and within the mortar and the grout (cohesion failure).

In order to measure the unrestrained, free shrinkage of the mortars, both tile adhesive and grout mortar were tested on standard prisms (4×4×16 cm) under (i) 90%, (ii) 70% and (iii) 35% rel. hum. After 28 days the shrinkage for the grouting mortar is (i) 0.21 mm/m, (ii) 1.78 mm/m and (iii) 2.77 mm/m, respectively, while the tile adhesive shrinks by (i) 0.36 mm/m, (ii) 1.72 mm/m and (iii) 2.39 mm/m. Both mortars show quite similar shrinkage. The shrinkage of the mortar sandwiched between the substrate and the tile is restrained and cannot shrink to the full extend observed in the case of the mortar prisms. The length changes during different storage conditions (dry, wet, alternating) were measured for the substrate and the tile on samples of the first setup (see Section 2.1.) [14,15]. These length changes were about one order of magnitude lower compared to those of the mortar prisms. Of special importance is the difference in shrinkage between the stiff tile and the substrate. Due to this differential length changes the interfaces between tile and mortar as well as between mortar and substrate are supposed to bare high stresses. The occurrence of aforementioned cracks at these locations indicates that the stress concentrations at the interface were above maximum adhesion strength inducing cracking.

Whether cracks form at the interface or within the mortar depends on the strength of the interfaces. Within samples in which the rear side of the tile is cleaned with a water high-pressure cleaner only, cracking mainly occurred at the interface (Figs. 7a,b and 12b,c). Thus, the interface can be interpreted in this case as the mechanically weakest structure. Cracks within the mortar, on the contrary, occurred in samples where the rear sides of the tile were abraded. We therefore

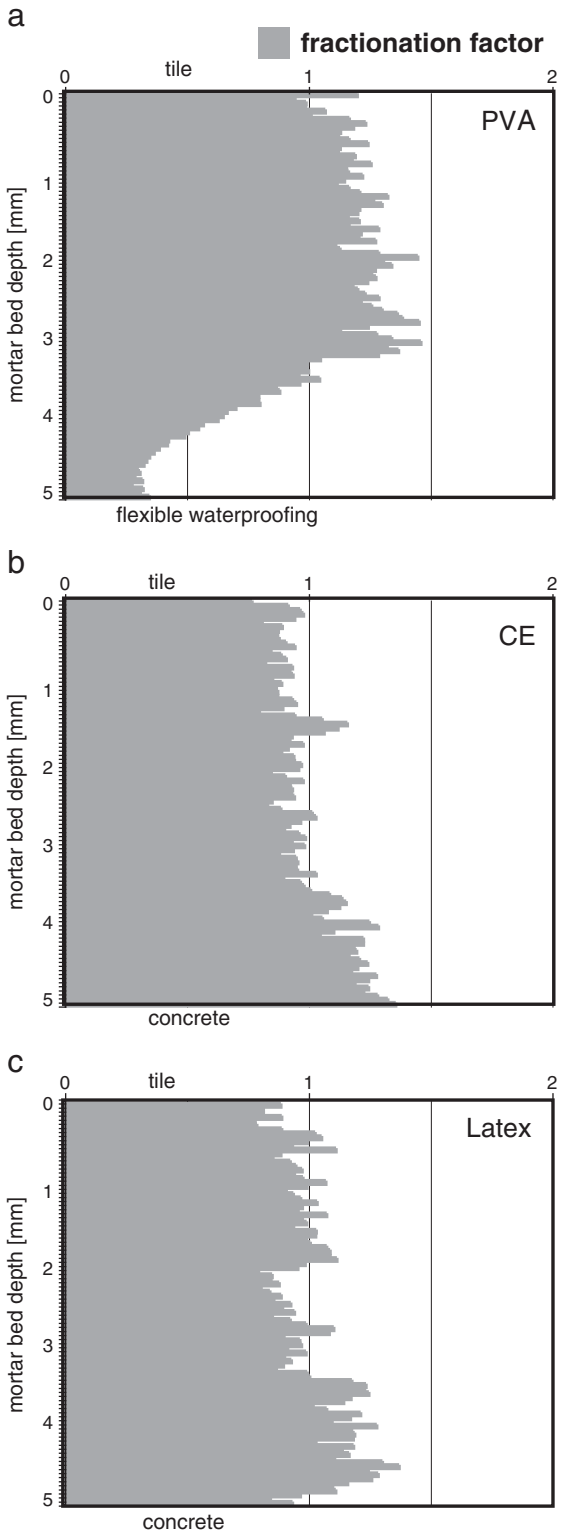

Fig. 10. Vertical distribution of (a) PVA (sample FW-dry), (b) CE (sample CO1-dry) and (c) latex (sample CO2-dry) within the mortar matrix at central positions after dry storage. The fractionation factor on the x-axes indicates depletion (<1) or enrichment of organic additives (>1).

assume that the abrasion destroys the glassy bottom face of porcelain allowing a direct connection of the applied mortar to the tile internal porosity. As a consequence, the adhesion between mortar and tile increased. Cohesion failure (vertical cracks) was already observed in the sample stored for 7 days only under dry conditions (Fig. 5), indicating that these vertical cracks primarily result from the early curing processes. Capillary shrinkage primarily affects vertical cracks during the dry storage.

4.2. Processes related to wet storage

During wet storage water can enter the system either along primary pathways or along pathways newly created during drying of the mortar. In the case of the "open" setup in sample NG (no grouts, no sealing of substrate) this assumption can be confirmed by hydrates, which mainly occurred along the interface between the mortar and the substrate and in the mortar in locations at the rim of the tile (Fig. 7c). Additionally, precipitates were observed in the vicinity of cracks indicating that these cracks acted as water pathways.

In samples with grouts applied and sealed substrate (FW and CO), the grouts are the only possible pathways for water to infiltrate into the mortar. The crack at the tile–grout interface observed in sample FW-wet on the right side towards the main (large) tile ends about 4 mm from the top of the grout (Fig. 7b). No connection between this crack and the crack at the tile–mortar interface is observed. No secondary formed minerals (hydrates, carbonates) were observed in the tile-mortar interface crack (FW-wet) suggesting that no significant amount of water entered the mortar along the grout during wet storage over 42 days. This assumption is confirmed by TGA and LSM measurements. Neither TGA analysis points to an enhanced degree of hydration (Fig. 11) nor do LSM images indicate remobilisation of soluble polymers in these regions (Fig. 9). On the contrary, hydrates in cracks at the tile–grout interface and in the pores near that crack indicate that water intruded the grout mortar along the new pathway generated by cracking.

Eventually a longer storage under wet conditions might lead to a connection of the crack at the tile–grout interface and the tile–mortar interface enabling water infiltration into the mortar. However, water infiltration into the mortar would lead to swelling (up to 0.5 mm/m) [18] generating a local expansion. The resulting stress rises might induce a propagation of the pre-existing cracks (Fig. 13). Additionally, cement hydration can restart, leading to chemical shrinkage. This creates additional internal porosity, refines the pore structure and may create an additional capillary tension during wetting and drying processes. This may increase shrinkage stresses, which can widen the pre-existing cracks and even cause formation of new vertical cracks (Fig. 14). In the context of a long-term field study such crack propagation scenarios were indeed observed in real systems exposed to outdoor weathering conditions [24]. Secondary minerals formed within those cracks in parts heal those cracks but mainly lead to widening of cracks during several weathering cycles and therefore weaken the system additionally [16].

5. Conclusions

Microstructures of the system tile–tile adhesive–substrate–grout mortar were studied in terms of local mechanical and microstructural variations on large-sized tiles (30×30 cm). Under controlled laboratory conditions, we investigated water percolation as a function of variation in experimental setup and water pathways generated by various shrinkage mechanisms.

Drying and hydration induce stress concentrations along mechanical anisotropies (interfaces) leading to cracks either within the mortar or at the interfaces of tile–mortar and tile–grout. These interfacial cracks interconnect the mortar with the surrounding environment (water/air, depending on storage conditions). Such cracks, mainly formed at rim positions, act as pathways for water infiltration during wet storage, or transferred to natural weathering conditions, infiltration of rainwater. Within our experiments, only a single cycle including drying and rewetting was investigated. Under outdoor weathering conditions, however, these drying–wetting cycles

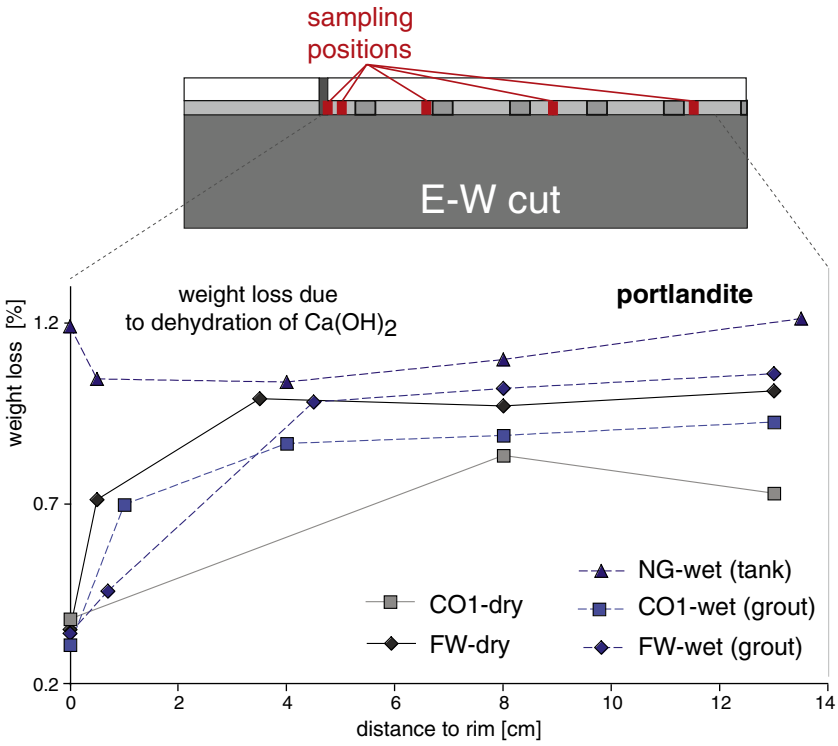

Fig. 11. Spatially resolved portlandite content for different storage conditions based on dehydration during thermogravimetric analysis (430 °C–480 °C).

repeat frequently during the time period of a year. With every cycle of swelling and shrinkage the system is stressed. The crystallisation of secondary hydrate phases, which was already observed after 6 weeks of wet storage in the laboratory experiments, may widen these cracks severely in the real system. Such a progression was observed in vertical cracks of sample NG-wet. While in this case the tile–mortar interface had a good adhesion due to abrasion of the rear side of the tile, untreated tiles would fail at this interface and entering water would affect crystallisation of secondary hydrates enhancing crack propagation. A typical damage on outdoor tilings develops over several years under alternating dry–wet and hot–cold conditions. In order to properly track down the evolution of a typical failure an appropriate field study was carried out [16]. Here the study of such alternating drying–wetting cycles indeed shows the progression of the initial failures demonstrated in the present study. The associated microstructural investigations indeed confirm the significance of our

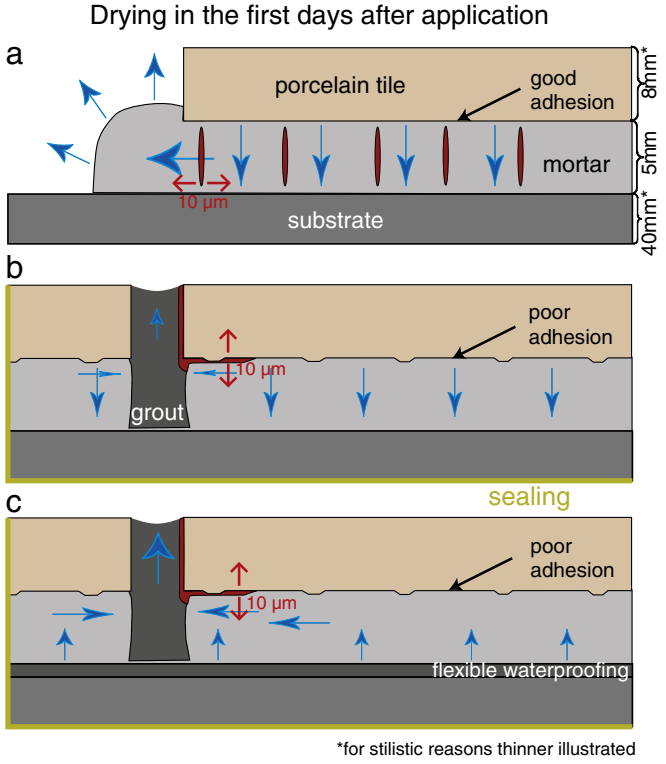

Fig. 12. Schematic drawing of water transport mechanisms in samples (a) without grouting (NG), (b) with grouts and sealed substrate (CO) and (c) with grouts, sealed substrate and a flexible waterproofing between substrate and mortar (FW).

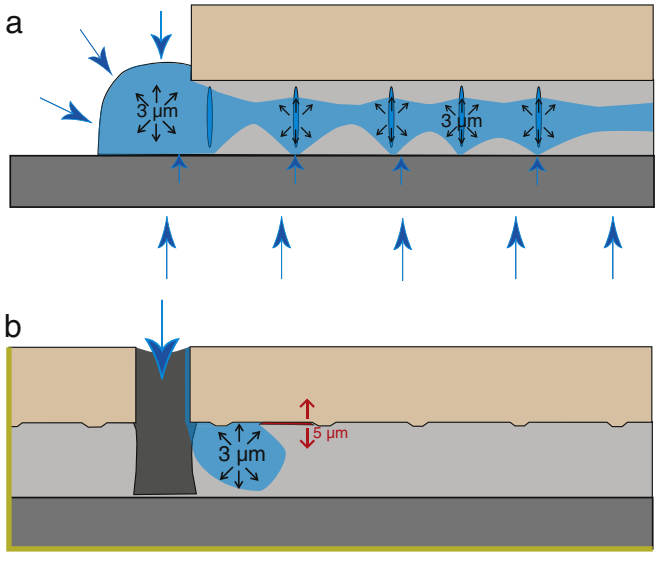

Fig. 13. Rewetting (a) directly over mortar and substrate (NG) or (b) along the grout (FW and CO). Mortar expansion due to water absorption and renewed cement hydration.

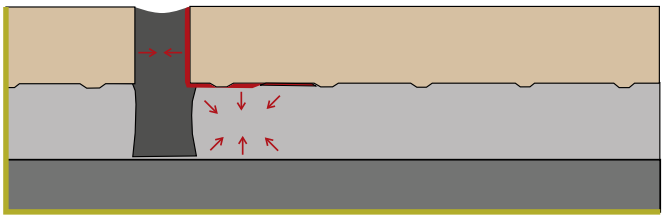

Fig. 14. Shrinkage of mortar by enhanced capillary shrinkage due to pore size reduction induced by secondary hydration. Existing cracks further widen or even propagate.

experimental study for real outdoor applications. Furthermore, they reveal that the structures observed in the present study reflect an early stage of failure evolution. Subsequent temperature and moisture cycles provoke further crack propagation, crack widening and hydration leading to severe failure of the tiled systems.

In order to avoid failures on the construction site several parameters like (i) the material choice (e.g. size and kind of tile material, appropriate tile adhesive), (ii) structural design (e.g. water drainage, flexible waterproofing) or (iii) appropriate installation practices (e.g. pre-treatment of substrate and tiles) need to be properly adjusted to each other and to the physico-chemical conditions of the framework.

Acknowledgements

The authors thank Josef Kaufmann (Empa) for helpful discussions. Hanspeter Waser is acknowledged for benefiting setup developments and assistance for experimental works. Financial support by the Swiss Commission for Technology and Innovation (CTI) is gratefully acknowledged (CTI project No. 8605.1 EPRP-IW).

References

[1] J. Felixberger, Einflussfaktoren auf den Haftverbund Untergrund - Fliese - keramischer Belag, in: J. Plank, D. Stehpan (Eds.), Tagung Bauchemie, GdCH-Fachgruppe Bauchemie, München, Germany, 2003, pp. 47–53.
[2] C.Y. Yiu, D.C.W. Ho, S.M. Lo, Weathering effects on external wall tiling systems, Constr. Build. Mater. 21 (2007) 594–600.
[3] J.D. Silvestre, J. de Brito, Ceramic tiling inspection system, Constr. Build. Mater. 23 (2009) 653–668.
[4] A.A.P. Mansur, O.L. Nascimento, H.S. Mansur, Data collection of five years of exterior facade pathologies in Brazil, IX World Congress on Ceramic Tile Quality, Logui Impresión, Castellon, Spain, 2006, pp. PBB107–PBB120.
[5] K. Pass, R. Zurbriggen, H. Waser, A. Wetzel, A. Greminger, M. Herwegh, J. Kaufmann, Mit Mikrorissen fängt es an, Fliesen und Platten 59 (10) (2009) 26–31.
[6] A.A.P. Mansur, O.L. do Nascimento, H.S. Mansur, Physico-chemical characterization of EVA-modified mortar and porcelain tiles interfaces, Cem. Concr. Res. 39 (2009) 1199–1208.
[7] Y. Ohama, Handbook of Polymer-Modified Concrete and Mortars, Properties and Process Technology, Noyes Publications, Park Ridge, New Jersey, 1995.
[8] K. Scrivener, H.H. Patel, P.L. Pratt, L.J. Parrott, Analysis of phases in cement paste using backscattered electron images, methanol adsorption and thermogravimetric analysis. Microstructural development during hydration of cement, in: L.J. Struble, P.W. Brown (Eds.), Materials Research Society Symposium Pittsburgh, 1986, pp. 67–76.
[9] A.A.P. Mansur, D.B. Santos, H.S. Mansur, A microstructural approach to adherence mechanism of poly(vinyl alcohol) modified cement systems to ceramic tiles, Cem. Concr. Res. 37 (2007) 270–282.
[10] A. Dimmig-Osburg, I. Pietsch, J. Pietsch, Polymer additives and their influence on the cement microstructure in the early stages of hardening, ZKG Int. 59 (2006) 72–83.
[11] A. Jenni, M. Herwegh, R. Zurbriggen, T. Aberle, L. Holzer, Quantitative microstructure analysis of polymer-modified mortars, J. of Microscopy-Oxford 212 (2003) 186–196.
[12] A. Jenni, L. Holzer, R. Zurbriggen, M. Herwegh, Influence of polymers on microstructure and adhesive strength of cementitious tile adhesive mortars, Cem. Concr. Res. 35 (2005) 35–50.
[13] F.L. Maranhao, V.M. John, Bond strength and transversal deformation aging on cement–polymer adhesive mortar, Constr. Build. Mater. 23 (2009) 1022–1027.
[14] A. Wetzel, R. Zurbriggen, M. Herwegh, Spatially resolved evolution of adhesion properties of large porcelain tiles, Cem. Concr. Compos. 32 (2010) 327–338.
[15] F. Winnefeld, J. Kaufmann, E. Hack, S. Harzer, A. Wetzel, R. Zurbriggen, Length changes of adhesive mortars and their impact on adhesion strength, to be submitted to construction and Building Materials.
[16] A. Wetzel, Mechanisms of shrinkage and adhesion failure of tile adhesive mortars, PhD-thesis, University of Bern, Bern, 2010.
[17] ZDB, ZDB leaflet — bonded waterproofing, 2005.
[18] A. De Gasparo, M. Herwegh, R. Zurbriggen, K. Scrivener, Quantitative distribution patterns of additives in self-leveling flooring compounds (underlayments) as function of application, formulation and climatic conditions, Cem. Concr. Res. 39 (2009) 313–323.
[19] A. Jenni, R. Zurbriggen, L. Holzer, M. Herwegh, Changes in microstructures and physical properties of polymer-modified mortars during wet storage, Cem. Concr. Res. 36 (2006) 79–90.
[20] G. Sant, P. Lura, J. Weiss, Measurement of volume change in cementitious materials at early ages — review of testing protocols and interpretation of results, Concrete Materials 2006, Natl Acad Sci, Washington, 2006, pp. 21–29.
[21] M. Geiker, T. Knudsen, Chemical shrinkage of Portland-cement pastes, Cem. Concr. Res. 12 (1982) 603–610.
[22] V. Slowik, E. Schlattner, T. Klink, Experimental investigation into early age shrinkage of cement paste by using fibre Bragg gratings, Cem. Concr. Compos. 26 (2004) 473–479.
[23] V. Slowik, M. Schmidt, R. Fritzsch, Capillary pressure in fresh cement-based materials and identification of the air entry value, Cem. Concr. Compos. 30 (2008) 557–565.
[24] R. Zurbriggen, A. Wetzel, A. Greminger, J. Kaufmann, K. Pass, H. Waser, Outdoor tile damages — a study on critical parameters and characteristic microstructures, in: F. Leopolder (Ed.), IDMMC, Drymix.info, Nürnberg, Germany, 2009, pp. 18–24.